Organic & Biomolecular Chemistry

Dynamic Article Links

Cite this: *Org. Biomol. Chem.*, 2012, **10**, 1459

www.rsc.org/obc

PAPER

Phosphole modified pentathienoacene: Synthesis, electronic properties and self-assembly†

Jun-Hua Wan,*[a] Wei-Fen Fang,[a] Yi-Bao Li,[b,c] Xu-Qiong Xiao,[a] Li-Hong Zhang,[a] Zheng Xu,[a] Jia-Jian Peng[a] and Guo-Qiao Lai*[a]

Received 16th September 2011, Accepted 17th November 2011
DOI: 10.1039/c1ob06584j

A series of new ladder π-conjugated materials, phosphole modified pentathienoacene (**PO-PTA**), are synthesized and characterized. Single-crystal X-ray results demonstrate that methyl-disubstituted **PO-PTA** forms a face-to-face dimer structure driven by π–π interactions. The investigations of optical properties showed that the oxidized phosphole moiety in this ladder system can effectively narrow the band gap. **PO-PTA** is a promising building block in π-conjugated polymers and oligomers for optoelectronic applications. The derivative of **PO-PTA**, obtained by introducing four long alkyl chains, can self-assemble into one-dimensional (1D) fibers based on intermolecular π–π interactions, dipole–dipole interactions and van der Waals interactions. Interestingly, the uniform and well-ordered monolayers were also obtained for **PO-PTA** derivative on a HOPG (highly oriented pyrolytic graphite) surface.

Introduction

Ladder π-conjugated systems with fused polycyclic skeletons are an important class of compounds for organic-electronic materials because of their effective extension of the π-conjugation without any conformational disorder.[1] Their rigid π-conjugated frameworks are suitable for forming dense molecular packing in the condensed phase, which can lead to intriguing electronic properties, such as high carrier mobility.[2] Furthermore, the fused aromatics as building blocks were usually introduced into π-conjugated polymers toward organic field-effect transistors (OFETs) and photovoltaic applications.[3]

Pentathienoacene (**PTA**) was attractive because it combined the molecular shape of pentacene, which leads to a favorable crystal packing geometry and orientation, with a thiophene monomer, which would increase stability and nuclear aromaticity and also provide points of attachment for solubilizing substituents.[2a,4] Very recently, a silole modified pentathienoacene (sila-pentathienoacene, **Si-PTA**) had been synthesized by us through replacing the central sulfur atom of **PTA** with a silylene moiety.[5] In this paper, we reported the synthesis of new conjugated heteroacene (***P*-PTA**: **2a** and **2b**) based on phosphorus-containing pentathienoacene by replacing the central sulfur atom of **PTA** with a P atom (see Scheme 1). The formed phosphole, a phosphorus-bridged cyclic butadiene, has a low-lying LUMO due to the effective σ* (*P*–R)–p*(1,3-diene) hyperconjugation,[6] giving rise

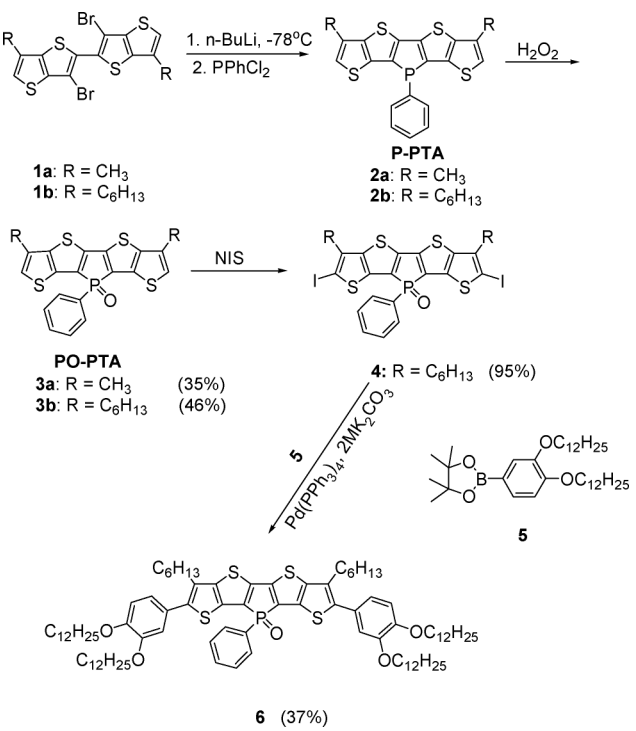

Scheme 1 The synthesis for compounds **3** and **6**.

[a]*Key Laboratory of Organosilicon Chemistry and Material Technology of Ministry of Education, Hangzhou Normal University, Hangzhou, 310012, P. R. China. E-mail: wan_junhua@hznu.edu.cn, gqlai@hznu.edu.cn; Fax: 86-571-28868081; Tel: 86-571-28868081*
[b]*National Center for Nanoscience and Technology, Beijing, 100080, China*
[c]*Key Laboratory of Organo-pharmaceutical Chemistry of Jiangxi Province, Gannan Normal University, Ganzhou 341000, Jiangxi Province, P. R. China*

† Electronic supplementary information (ESI) available: The POM, OM and SEM images of gel, ^{1}H NMR spectra. CCDC reference number 822000. For ESI and crystallographic data in CIF or other electronic format see DOI: 10.1039/c1ob06584j

to intriguing electronic structures. More importantly, the LUMO level was further reduced through oxidation of the central phosphorus center of ***P*-PTA** and achieved their oxidized relatives (**PO-PTA**: **3a** and **3b**) with quite high thermal stability. Compared to benzo-condensed dithieno[3,2-b:2′,3′-d]phospholes,[6c] two terminal thiophene rings of **PO-PTA** provide an opportunity to be chemically modified for functionalization.

Current demands in the area of organic semiconductor design focus on both electronic properties and self-assembling ability in order to create well-defined nanostructures. Self-assembly presents a process for controlling the supramolecular packing and orientation of molecules to obtain the ordered aggregates in materials sciences.[7] The optical and electronic properties of organic functional materials, which depend to a certain extent on the molecular packing arrangements through excitonic interactions, can be effectively modulated by self-assembly.[8] Recently, low molecular weight organogelators (LMOGs) as a novel class of self-assembled materials have attracted much attention, which produce one-dimensional (1D) stacks of functional molecules and are easily processable without using advanced techniques.[9,10] Self-organized 1D supramolecular structures offer great potential in optoelectronic applications, such as field effect transistors (FET)[11] and photovoltaics (PV),[12] because of their enhanced device performance. This demand inspired us to introduce four long alkyl chains into phosphorus-containing pentathienoacene to obtain the **PO-PTA** derivative (**6**). The self-assembly behaviors for compound **6** in different conditions (in organic solvent and liquid-solid interface) were investigated.

The obtained interesting ladder π-conjugated materials (**PO-PTA**) have a much smaller band gap (2.48 eV) than those of **PTA** (3.20 eV) and **Si-PTA** (2.76 eV). The fused polycyclic skeletons of this system are inclined to form a face-to-face stacked structure through π–π interaction and dipole–dipole interaction. Like **DTS**[3a,d] and β-alkylsubstituted fused thiophene,[3g] **PO-PTA** is also a promising building block in π-conjugated polymers and oligomers for FET and photovoltaic applications. In addition, **PO-PTA** bearing long alkyl chains can self-assembly into different aggregates, such as one-dimensional (1D) fibers and a two-dimensional (2D) molecular adlayer. This serves as an excellent example, demonstrating the fabricating of well-defined nanostructure from π-conjugated ladder system.

Experimental

General methods

All starting materials were obtained from commercial suppliers and used as received. Reagent grade solvents were dried and purified according to the following procedures: THF was dried over sodium metal and distilled. Compounds **1**[4,5] and **5**[13] were synthesized according to reported methods.

NMR spectra were recorded on a Bruker DPX 400 (^{1}H NMR 400 MHz and ^{13}C NMR 100 MHz) spectrometer. Matrix-assisted laser desorption ionization time-of-flight (MALDI-TOF) mass spectra were obtained using 2, 5-dihydroxybenzoic acid (DHB) as the matrix on a Perseptive Biosystems Voyager DESTR MALDI-TOF mass spectrometer. Cyclic voltammetry was carried on a CHI 600A potentiostat. The working and reference electrodes were disk Pt and Ag/$AgNO_3$ (0.1 M in acetonitrile), respectively. The luminescence spectra were measured on a Hitachi F-2700 fluorescence spectrophotometer (the path length of the quartz cell is 1 cm). The emission band-width was 3 nm. UV absorption spectra were obtained using a scinco S-3150 UV–vis spectrophotometer. POM images were recorded on an E600POL (Nikon Corp). FE-SEM images of xerogels were obtained using FEI Sirion-100 (Philips) with accelerating voltage 25.0 kV. The samples were prepared by dropping the gels on a flat surface of a cylindrical brass substrate and coating with Au. STM measurements were performed by using a Nanoscope IIIa (Veeco Metrology, USA) with mechanically formed Pt/Ir (80/20) tips. A droplet (2 μL) of their 1-phenyloctane solutions was deposited on freshly cleaved HOPG surface and immediately observed by STM with constant current mode. The proposed models of molecular patterns were constructed using HyperChem. HOPG (grade ZYB) was purchased from Veeco Metrology (USA). Diffraction data of single crystal were obtained with Mo_{Ka} ($\lambda = 0.71073$ nm) at 293 K using an Oxford Diffraction X-Calibur CCD system.

Crystal data for 3a. $C_{20}H_{13}OPS_4{\cdot}CHCl_3$, M = 547.88, orthorhombic, $a = 20.6692(4)$ Å, $b = 7.93121(18)$ Å, $c = 29.3363(8)$ Å, $\alpha = 90.00°$, $\beta = 90.00°$, $\gamma = 90.00°$, $V = 4809.15(19)$ Å^3, T = 293(2)K, space group $Pca21$, $Z = 8$, 35391 reflections measured, 8740 independent reflections ($R_{int} = 0.0452$). The final R_1 values were 0.0576 ($I > 2\sigma(I)$). The final $wR(F^2)$ values were 0.1410 ($I > 2\sigma(I)$). The final R_1 values were 0.0737 (all data). The final $wR(F^2)$ values were 0.1509 (all data). The goodness of fit on $F2$ was 1.025. CCDC number CCDC 822000. These data can be obtained free of charge from The Cambridge Crystallographic Data Centre at www.ccdc.cam.ac.uk/data_ request/cif.

Synthesis of compound 3a. To a solution of **1a** (0.24 g, 0.52 mmol) in 150 mL THF, *n*-BuLi (0.44 mL, 1.09 mmol) was added dropwise at −78 °C and stirred for 20min. Then, $PPhCl_2$ (0.10 g, 0.57 mmol) was added dropwise to the solution at this temperature, and the solution was quickly warmed to room temperature and stirred for 2 h. After evaporating most of the THF, the mixture was dissolved into diethyl ether and washed with water and dried over anhydrous $MgSO_4$. The solvent was removed under vacuum, the obtained residue taken up in dichloromethane and filtered over neutral alumina. The filtrate was dried under vacuum to afford orange amorphous powder. The obtained mixture was oxidized with H_2O_2 and stirred at room temperature for another hour, and the solvent was removed under vacuum. The residue was extracted with dichloromethane and the organic layer was dried with $MgSO_4$, and the solvent was removed under vacuum. The solid was taken up in *n*-hexane, heated for 10 min, and filtered. The product **3a** was obtained as a red solid in 35% yield. mp:178–180 °C. ^{1}H NMR (400 Hz, $CDCl_3$): δ 7.83 (q, J = 7.2 Hz, 2H), 7.53 (t, J = 6.0 Hz, 1H), 7.45–7.25 (m, 2H), 6.99 (s, 2H), 2.37 (s, 6H, –CH_3); ^{13}C NMR (100 Hz, $CDCl_3$): δ 147.5, 147.2, 143.5, 136.4, 132.8, 130.8, 129.9, 129.2, 192.1, 123.7, 14.7 ppm. ^{31}P NMR ($CDCl_3$): δ 17.85 ppm. MALDI-TOF/DHB-HRMS calcd for $C_{20}H_{13}OPS_4$: m/z (+H$^+$): 428.9660. Found: m/z (+H$^+$): 428.9661.

Synthesis of compound 3b. Compound **3b** was prepared according to a similar procedure to **3a**. The product **3b** was obtained as a red solid in 46% yield.mp:133–135 °C.^{1}H NMR (400 Hz, $CDCl_3$):δ 7.85 (q, J = 7.2 Hz, 2H), 7.53 (t, J = 6.0 Hz, 1H), 7.46–7.26 (m, 2H), 6.99 (s, 2H), 2.70 (t, J = 7.2 Hz, 4H), 1.74

(t, J = 7.2 Hz, 4H), 1.34–1.33 (m, 12H), 0.89 (s, 6H, CH_3); ^{13}C NMR (100 Hz, $CDCl_3$): δ 147.2, 142.4, 136.4, 135.3, 132.8, 130.8, 129.7, 129.2, 128.5, 122.9, 31.4, 29.7, 29.0, 29.6, 22.6, 14.1 ppm. ^{31}P NMR ($CDCl_3$): δ 18.05 ppm. MALDI-TOF/DHB-HRMS calcd for $C_{30}H_{33}OPS_4$: m/z (+H^+): 569.1225. Found: m/z (+H^+): 569.1217.

Synthesis of compound 4. To a solution of **3b** (0.568 g, 1 mmol) in dichloromethane/acetic acid (1 : 1, 25 mL) *N*-iodosuccinimide (0.675 g, 3 mmol) was added at 0 °C. After 2.5 h sodium thiosulfate (10% aq., 20 mL) was added and the product was extracted to diethyl ether (20 mL), washed with additional sodium thiosulfate (10%, aq., 20 mL), sodium carbonate (sat. aq., 20 mL) and finally water (20 mL). The organic layer was dried with $MgSO_4$ and the solvent was removed under vacuum. The obtained red solid was purified by column chromatography (silica gel, hexane/DCM = 3 : 1, v/v) to give pure **4** as a red solid in 95% yield. mp:200–203 °C. ^1H NMR (400 Hz, $CDCl_3$):δ 7.78 (q, J = 7.2 Hz, 2H), 7.56 (t, J = 6.0 Hz, 1H), 7.47–7.45 (m, 2H), 2.70 (t, J = 7.2 Hz, 4H), 1.67 (t, J = 7.2 Hz, 4H), 1.38–1.32 (m, 12H), 0.90 (t, 6H) ppm.^{13}C NMR (100 Hz, $CDCl_3$): δ146.6, 146.4, 140.5, 139.8, 138.9, 133.1, 130.7, 129.3, 31.7, 31.5, 29.0, 28.3, 22.6, 14.1. ^{31}P NMR ($CDCl_3$): δ 17.34 ppm. MALDI-TOF/DHB-HRMS calcd for $C_{30}H_{33}OPS_4I_2$: m/z (+H^+): 820.9157. Found: m/z (+H^+): 820.9165.

Synthesis of compound 6. Compounds **4** (1.3 g, 1.58 mmol) and **5** (2.8 g, 4.75 mmol) were dissolved in toluene (15 mL) and K_2CO_3 (2 M, aq., 7 mL). After adding a catalytic amount of $Pd(PPh_3)_4$ (0.03 g, 0.02 mmol), the reaction mixture was refluxed at 75 °C for 24 h. The product was extracted with CH_2Cl_2 and the combined organic layer was washed by water, brine, and dried over $MgSO_4$. The solvent was removed under vacuum and the residue was purified by column chromatography (silica gel, hexane/ethyl acetate = 6 : 1, v/v) to give the title product as a red solid in 37% yield. Mp: 76–78 °C. ^1H NMR (400 Hz, $CDCl_3$): δ 7.88 (q, J = 7.2 Hz, 2H), 7.54 (t, J = 6.0 Hz, 1H), 7.47–7.43 (m, 2H), 6.96–6.89 (m, 6H), 4.01 (t, J = 6.4 Hz, 8H), 2.78 (t, J = 7.2 Hz, 4H), 1.83–1.72 (m, 8H), 1.59–1.58 (m, 4H), 1.47–1.25 (m, 84H), 0.88 (t, 18H); ^{13}C NMR (100 Hz, $CDCl_3$): δ149.28, 148.99, 143.59, 141.21, 134.24, 130.91, 130.80, 130.42, 129.24, 129.10, 126.96, 121.97, 114.92, 113.59, 69.37, 69.29, 31.93, 29.65, 29.08, 26.05, 22.69, 22.59, 14.06 ppm; ^{31}P NMR ($CDCl_3$): δ 18.19 ppm. MALDI-TOF/DHB-HRMS calcd for $C_{90}H_{137}O_5PS_4$: m/z: 1456.9086. Found: m/z: 1456.9107.

Results and Discussion

Synthesis

Scheme 1 depicts the synthetic route to phosphorus-pentathienoacenes (**3**) and their derivative (**6**). A key intermediate **1** was synthesized using the reported methodology. The corresponding phospholes (**2**, ***P*-PTA**) were obtained according to the classical method from compound **1**. Thus, compound **1** was treated with two equivalents of *n*-BuLi to produce the corresponding dianion, which was then quenched with $PhPCl_2$. The attained air-unstable ***P*-PTA** were directly transferred to their oxidized relatives (**3**, **PO-PTA**) by oxidation of the central phosphorus atom with H_2O_2. By introducing hexyl chains on two terminal thiophene rings, the soluble phosphorus-pentathienoacene (**3b**) was obtained. However, as well as for comparison, the other one with two methyl groups (**3a**) was also synthesized to get a single crystal for explaining the molecular packing structure of the π-conjugated ladder system in solid state.

Generally, the synthesis of the phosphole derivatives (**6**) involves three procedures, *i.e.*, synthesis of corresponding diiodo-funtionalized compound **4**, synthesis of the 3,4-dialkoxyphenyl pinacolboronic ester **5**, and coupling reaction (see Scheme 1). Double iodination of phosphole **3b** was achieved by treatment with excess *N*-iodosuccinimide (NIS) to afford **4** in high yields after purification through column chromatography. 3, 4-dialkoxyphenyl pinacolboronic ester (**5**) was synthesized according to the literature.[13] Compound **4** then underwent 2-fold Suzuki coupling reactions with the 3, 4-dialkoxyphenyl pinacolboronic ester to afford the corresponding 2-fold substituted **PO-PTA** derivatives **6** in acceptable yields. The structure and purity of the phosphole **3** and its derivative **6** compound system were confirmed by ^1H NMR, ^{13}C NMR and ^{31}P NMR, MALDI-TOF-HRMS.

Crystal structure

Single crystals of **3a** suitable for X-ray analysis were obtained by slow evaporation from $CHCl_3$ at room temperature. As shown in Fig. 1, the molecular structure of **3a** shows that the ring skeleton is highly planar. In the crystal structure, two inversion-related molecules associate through π–π interactions (centroid.....centroid = 3.63 Å) to form a face-to-face dimer. It is worth noting that the significant interactions between divalent S atoms and substituting phenyl rings (S . . . π interaction), usually occurring in protein crystal structures by promoting the formation of α-helices, were recognized in this crystal structure.[14] Therefore, it is convincible that the S . . . π interaction also plays an important role in stabilizing molecular dimer structure for forming above-mentioned face-to-face arrangement. Interestingly, the molecular dimers interconnect pairwise through π–π interactions

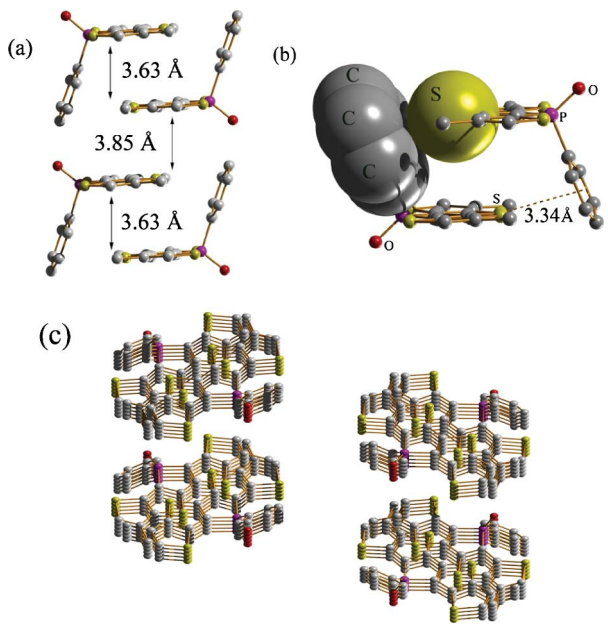

Fig. 1 The crystal packing of **3a**. (a) side view; (b) side view for S . . . π interactions; (c) molecular arrangement in single crystal.

(centroid . . . . .centroid = 3.85 Å) interactions to form an infinite chain along the axis. Intermolecular interaction is increased by a face-to-face arrangement of the conjugated molecules thus beneficial for achieving high carrier mobility.

The packing structure of **3a** in the solid state is obviously different from that of oxidized benzo-condensed dithieno[3,2-b:2′,3′-d]phospholes, which exhibits an edge-to-face herringbone-type arrangement of molecules in its solid state.[6c]

Gelation

Owing to bearing four long alkyl chains, compound **6** was evaluated for gelation properties in various organic solvents at a moderate concentration. The "stable to inversion of a test tube" method was adapted to test their gelation properties.[15] Generally, the gelation process involves three steps. The first is mixing an organogelator with a solvent at ambient temperature. The second is warming the mixture to produce a clear solution. Finally, the solution is cooled slowly to the ambient temperature. Gelation typically occurred during the cooling step. Compound **6** is readily soluble in chloroform, CH_2Cl_2, and THF, but it isinsoluble in some alcohol and alkane solvents. Among various solvents investigated here, only acetone and ethyl acetate were induced into gelation by the above method (see Table 1). Like most reported organogels, the organogels of **6** in acetone and ethyl acetate also exhibit thermally reversible sol–gel transitions. The data of the critical gelation concentration (CGC) for different solvents of the two compounds are shown in Table 1. The driving forces for gelation will be discussed below.

Aggregation structure of the gels

The morphology of xerogels of **6**, which are prepared by slow evaporation of acetone from the corresponding organogels, was investigated by optical microscopy (OM), polarized optical microscopy (POM), field emission scanning electron microscopy (FE-SEM) and atomic force microscopy (AFM). As shown in Fig. 2, the xerogels of compounds **6** are composed of fibrous structures. It is very interesting that the fibers of xerogels formed many spherical structures with different sizes from the OM images (Fig. 2b). The typical Maltese cross extinction (birefringence) observed under POM reveals that the fibers further aggregate into spherical crystallites (Fig. 2c). A more interesting possibility to grow spherical crystallites from an organogel is rarely realized.[16] The FE-SEM investigations provided the details of morphology of the xerogels. As shown in Fig. 2d, the spherical domains composed fibers can also be observed. The intertwisted and interlocked fibers formed the 3D network structure, as revealed by the large scale FE-SEM image (Fig. 2e), project from a central core. According to the AFM image (Fig. 2f), an observed fiber bundle is approximately 0.5 μm wide and incorporates several small fibers. The small fiber diameter ranged from 100 to more than 200 nm, suggesting that the observed small fibers are actually bundles of smaller fibers. It is obvious that the original fibers, aggregates formed from compound **6**, proceed to self-assemble into small fibers then the observed fiber bundles, which forms the backbone of the organogel. Based on the obtained results and the available literature,[17] the mechanisms

Table 1 Gelation properties of **6** in various solvents[a]

	6	
Solvents	state	CGC (mg mL^{-1})
hexane	P	
chloroform	S	
CH_2Cl_2	S	
THF	S	
toluene	S	
acetone	G	6
ethanol	P	
ethyl acetate	G	7

[a] G = gel, S = Solution, P = solution when heated but precipitation after cooling.

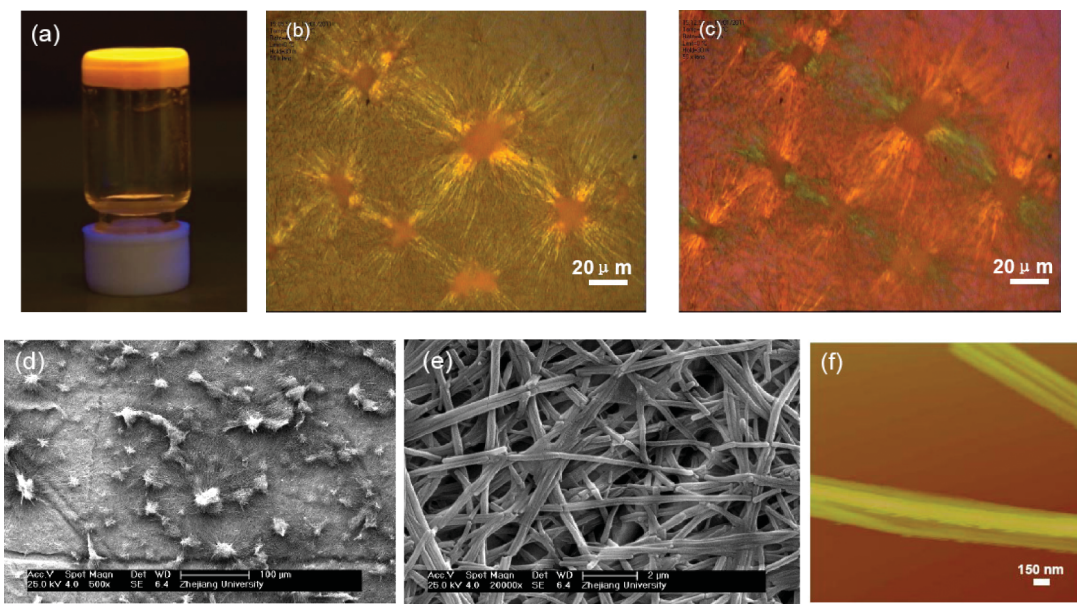

Fig. 2 (a) Photographic images of a gel of **6** in acetone observed upon UV irradiation at 365 nm. (b) OM image and (c) POM image, (d and e) FE-SEM images and (f) AFM image of a xerogel formed from **6** in acetone (6 mg mL^{-1}).

of gelation can be suggested: the gelation of compound **6** with acetone arises from a multistep process involving (i) the formation of nuclei, (ii) the growth of branched fibers from these nucleation points, and (iii) the formation of a three-dimensional network *via* the entanglement of dendritic-shaped crystallites.

Optical properties

UV-vis absorption and fluorescence characteristics of the new ladder compounds **3a** and **3b** were studied in both solution and solid state. As for compound **6**, the optical properties in the gel state were also investigated besides those in solution.

UV/Vis absorption spectra of **3a** and **3b** in toluene solutions and thin films prepared by a drop-casting method are shown in Fig. 3. In solution, both **3a** and **3b** showed two distinct absorption bands with maxima at 293 and 425 nm. The lower transition (425 nm) of **3a** and **3b** are observed at longer wavelength than the corresponding transition (392 nm) of **Si-PTA** implying that oxidized phosphole moiety in compounds **3** effectively narrows the HOMO–LUMO gaps of their fused π systems (Fig. 3a,b). The band gap from the absorption edge is around 2.48 eV, which is remarkably lower than those of **PTA**[2a] and **Si-PTA**[5].

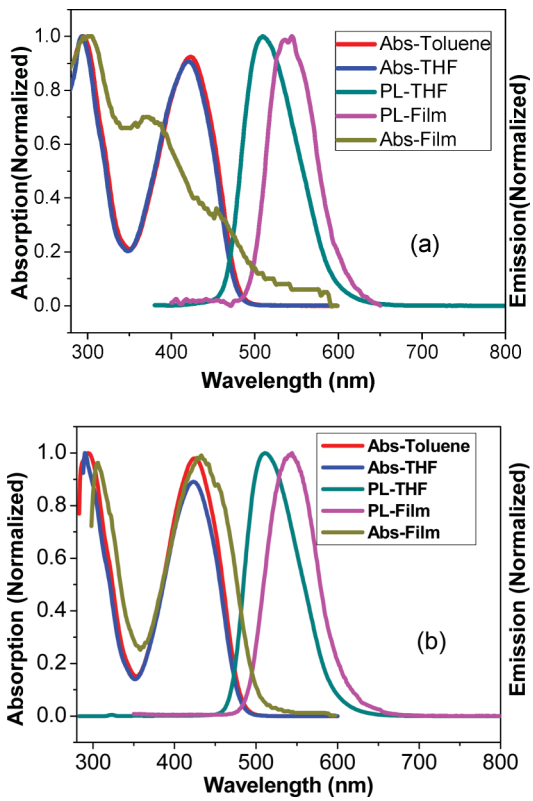

Fig. 3 Absorption and photoluminescence spectra of (a) **3a** and (b) **3b** in different environments. The concentration of all the solutions is kept to be 1×10^{-4} M. The films were prepared by drop-casting from a solution of toluene.

The absorption spectra of the films of **3b** are similar to the corresponding spectra in toluene solution, but show a slight red-shift and clear broadening compared to those in solution, suggesting the existence of weak intermolecular interaction. However, a large blue-shift (54 nm) and clear broadening were observed for compound **3a** with same comparison. The single crystal structure of **3a** shows there exists a significant π–π stacking. Based on the exciton-coupling theory, H-aggregates with face-to-face stacking result in a pronounced blue shift of the absorption and remarkable spectrum broadening.[18] Apparently, this point is consistent with its crystal structure. There is no dependence of the absorption maxima on the solvent polarity. The spectrum of **3a** and **3b** in THF is the same as that in toluene.

Similarly, compound **6** in solution also showed two distinct absorption bands with maxima at 321 and 462 nm (Fig. 4). The remarkable red-shifts of absorptions compared with that of **3a** and **3b** attributed to the presence of synthetic modification of the chromophore. Compared with the absorption of CH_2Cl_2 solution, the absorption of gel for **6** exhibits a significant blue-shift with two absorption bands at 270 nm and 440 nm, respectively.

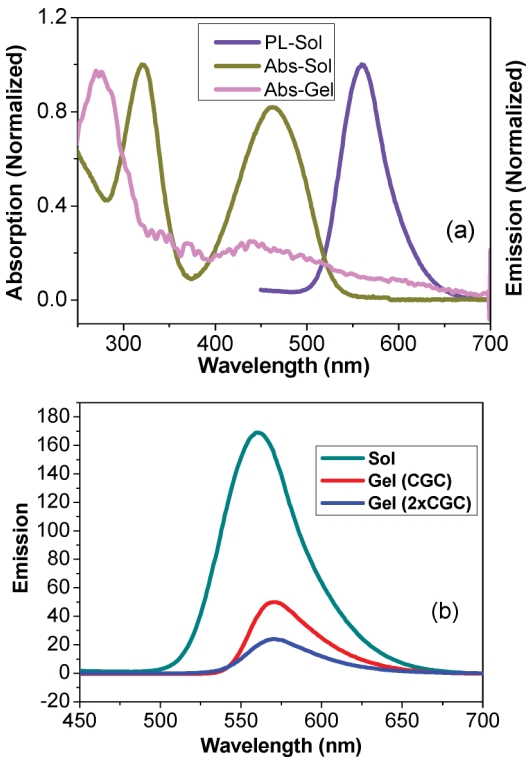

Fig. 4 (a) Absorption and photoluminescence spectra of **6** in different environments, solution and gel. The concentration of the solutions is kept to be 1×10^{-4} M. The concentration of the gel is 6 mg mL^{-1}. (b) Photoluminescence spectra of **6** in CH_2Cl_2 solution and gel with different concentration.

The large blue-shift for absorption with spectrum broadening is the typical features of H-aggregates and strongly suggests the existence of intermolecular π–π interaction in the gel state. Therefore, the π-stacking as one of driving forces may play a key role in the formation of organogels.

In toluene, compound **3a** and **3b** exhibit only one maximum emission at around 514 nm with high fluorescence quantum yields (0.58 for **3a** and 0.51 for **3b**). The emissions of films showed obvious red shifts (31 nm) in comparison with those in solution. Generally, the large red-shift of emission can be attributed to the extension of π-conjugation due to planarizartion of the molecular skeleton or the intermolecular interaction due to the aggregation (π-stacking),

Table 2 Photophysical data and dipole moment for compounds **3a**, **3b** and **6**

	Absorption (nm)[a]			Emission (nm)[a]			
Compound	Non-polar solvent	Polar solvent	Film/Gel	Non-polar solvent (Φ_f)[b]	Polar solvent	Film/Gel	μ (Debye)[c]
3a	293, 425	291, 420	301, 371	514 (0.58)	511	542	6.46 [d]/5.19
3b	293, 425	290, 423	303, 431	514 (0.51)	511	542	5.50
6	321, 462		270, 440	559		567	3.59

[a] Measured in solution (1×10^{-4} M) and in solid thin film on quartz plates prepared by spin-coating from toluene solution for **3a** and **3b** (non-polar solvent: toluene and polar solvent: THF), measured in solution (non-polar solvent: CH_2Cl_2) (1×10^{-4}M) and in gel of acetone with 6 mg mL^{-1} for **6**. [b] Fluorescence quantum yield relative to 9,10-diphenylanthracene in cyclohexane. [c] The dipole moments were obtained on a full optimization calculated on HF/6-31G(d,p) level based pm3 optimization geometry. [d] The dipole moment was obtained by carrying out a single point calculated at HF/6-31G(d,p) level based on the geometry obtained from crystal structure.

maybe both. Ladder π-conjugated systems have fused polycyclic skeletons, which are highly planar. It is reasonable to believe that the intermolecular interactions play a dominating role in the red-shift of emissions.

The dilute solution of **6** exhibited only one fluorescence maximum with λ_{max} at 559 nm. However, the slight difference is detected for the fluorescence spectra between the gel and solution. The emission for gel with λ_{max} at 567 nm exhibited a small red shift (8 nm) compared with that of the solution. As expected, the intensity of the emission of **6** in the gel state was obviously reduced as a result of the formation of H-aggregate. The relative absorption and emission data were listed in Table 2.

The molecules have an oxidized phosphole ring, creating the directional arrangement of its local dipole. The extensive calculations on dipole moment of model-ring systems, **3a**, **3b** and **6** were performed by using the Gaussian 03 program.[19] The dipole moment for **3a** were obtained by carried out a single point calculated at HF/6-31G(d,p) level based on the geometry obtained from the crystal structure. Similar data for **3b** and **6** were obtained on a full optimization calculated on HF/6-31G(d,p) level based pm3 optimization geometry. The long alkyl group was displaced by a hexyl group in order to reduce calculation time. The dipole moments are listed in Table 2. All model compounds have fairly large dipole moments. Upon aggregating, the fused polycyclic skeletons containing oxidized phosphole rings in this system tend to accept the inverse and face-to-face array due to the local dipole interactions. This fact is excellently in accordance with the single crystal structure for compound **3a**. Therefore, it is reasonable to consider that dipole–dipole interactions also play an important role in the formation of aggregates for all three compounds (**3a**, **3b**, **6**).[20]

In the case of the gel of compound **6**, intermolecular hydrogen bonding does not exist and other strong secondary interactions are believed to serve as the main driving forces for gelation, which contains intermolecular π–π interactions, dipole–dipole interactions and van der Waals interactions between the outside long alkyl chains.

Electrochemical properties

Due to the negligible effect on electronic properties from peripheral alkyl substitutes, only the redox properties of compound **3a** were investigated. The redox properties of **3a** were determined by cyclic voltammetry in solutions (1 mm) of tetrabutyl-ammonium hexafluorophosphate ($TBAPF_6$, 0.1 m) using a Pt wire as the counter electrode and a $Ag/AgNO_3$ (0.1 m) as the reference electrode. The cyclic voltammograms are given in Fig. 5.

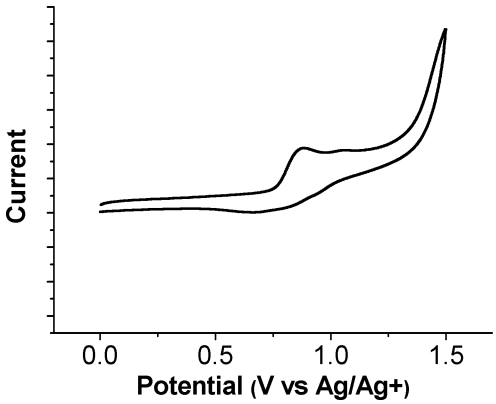

Fig. 5 Cyclic voltammograms of **3a** in CH_2Cl_2 for oxidation. Scan rate: 100 mV s^{-1}.

On sweeping anodically, **3a** undergoes two ireversible oxidation peaks. The oxidation potential with E^{Ox}_{onset} is 0.73 V (*vs* Ag/Ag^+) and obviously shifted negatively compared with that of oxidized benzo-condensed dithieno[3,2-b:2′,3′-d]phospholes, which shows ambipolar behavior with an irreversible oxidation at E_{ox} = 1.61 V (*vs.* Ag/AgCl).[6c] The HOMO energy level of **3a** is estimated from the onset of oxidation wave to be −5.43 eV based on the referenced energy level of Ag/Ag^+ (4.7 eV below the vacuum level). Compared with the HOMO of **PTA** (−5.33 eV)[2a] and **Si-PTA** (−5.21 eV),[5] the slight enhancement of HOMO level for **3a** may be ascribed to the increased electron-acceptor character of the phosphorus center. Unexpectedly, no invisible reduction peak in **3a** is detected. The reduction potential of **3a** was estimated from the difference between oxidation potential and optical band gap (2.48 eV). Therefore, the LUMO level can be obtained −2.95 eV, which is clearly lower than that of **Si-PTA** (−2.38 eV). Apparently, the oxidized phosphole moiety exerts a significant impact on LUMO levels.

2D self-assembly

Scanning tunneling microscopy (STM) is a powerful method to investigate the 2D assembly of functionalized organic molecules on surfaces, which provides access to supramolecular structures at the single molecule level.[21] For this purpose, compound **6** was investigated at the liquid–solid interface.

Compound **6** self-assembled into well-ordered monolayers when adsorbed from 1-phenyloctane on the HOPG (highly oriented pyrolytic graphite) surface, as shown in Fig. 6. From the large scale

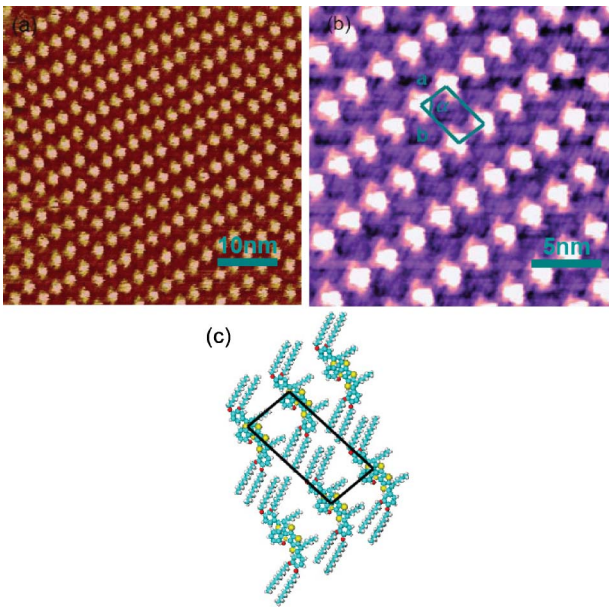

Fig. 6 (a) A large-scale STM image (55 nm × 55 nm) of **6**. (b) A high-resolution STM image (20 nm × 20 nm) of **6**. (c) The proposed structural model of the ordered array.

STM images of the adlayer, it is noticed that the remarkably bright spots were arranged uniformly in the whole area. The details of the adlayers were seen in the high-resolution STM images (Fig. 6b). Since bright STM images usually stem from strong adsorption of π-conjugated molecules on HOPG surface, the bright spots were assigned to the adsorption of the fused polycyclic skeletons of compound **6** with their molecular planes parallel to HOPG. The length of each bright spot is about 2.0 ± 0.2 nm, in agreement with the theoretical value of the π-conjugated backbone of compound **6** (2.1 nm). The relatively darker parts corresponded to the parallel alkyl chains with lower electronic density. Based on the high-resolution images, two piles of consecutive alkyl chains at the two ends of **6** aligned with a *trans* conformation, and the alkyl chains are aligned in a comb-like fashion between neighboring molecules and interdigitated with each other. On the basis of the above analysis, the unit cells of the adlayers are outlined in Fig. 6b. The lattice parameters were determined from the STM images to be $a = 2.8 \pm 0.1$ nm, $b = 4.2 \pm 0.2$ nm, and $a = (84 \pm 2)°$. The proposed models for the molecular arrangement models are illustrated in Fig. 6c.

It is well known that the formation of well-defined adlayer comes from the balance between molecule-substrate matching-interaction (adsorption energy) and molecule–molecule interactions, such as alkyl–alkyl interdigitation and head-group interactions. Generally, the interactions between long alkyl chains and substrate are very strong.[22] The formation of the adlayer for compound **6**, shown in Fig. 6, appears to be driven, primarily, by both adsorption energy and alkyl chain interdigitation, which determines the detailed assembly configuration of molecules.

Conclusions

A new series of ladder π-conjugated materials, phosphorus-containing pentathienoacene (**PO-PTA**), are synthesized and characterized. The band gap from the absorption edge is around 2.48 eV, which is remarkably lower than those of **PTA** and **Si-PTA**. The different investigations showed that the fused polycyclic skeletons of this system inclined to form face-to-face stacked structure through π–π interaction and dipole–dipole interaction. The novel π-conjugated system is a good candidate as a building block incorporated to π-conjugated polymers for FET and photovoltaic applications. Interestingly, the derivatives of **PO-PTA**, obtained by introducing long alkyl chains, can self-assembly into different supramolecular structures, such as 1D fibers and 2D monolayers. This study serves as an excellent example, demonstrating the fabricating of well-defined nanostructure from ladder π-conjugated materials.

Acknowledgements

This Project was supported by Zhejiang Provincial Natural Science Foundation of China (Y4110460) and MOE Key Laboratory of Macromolecular Synthesis and Functionalization, Zhejiang University (2010MFS03). We also thank Dr Lian-Bin Wu, Prof. Hua-Yu Qiu and Prof. Li-Jin Shu (*Hangzhou Normal University*) for his helpful discussion, Prof. Chen Wang (*National Center for Nanoscience and Technology*) for his help of the STM measurement, Prof. Wan-Zhi Chen (*Zhejiang University*) for his helpful discussion of single crystal structure.

References

1 (*a*) A. Fukazawa and S. Yamaguchi, *Chem.–Asian J.*, 2009, **4**, 1386–1400; (*b*) U. Scherf, *J. Mater. Chem.*, 1999, **9**, 1853–1864; (*c*) M. D. Watson, A. Fechtenköter and K. Müllen, *Chem. Rev.*, 2001, **101**, 1267–1300; (*d*) M. Bendikov, F. Wudl and D. F. Perepichka, *Chem. Rev.*, 2004, **104**, 4891–4946; (*e*) R. G. Harvery, *Polycyclic Aromatic Hydrocarbons*, Wiley-VCH, New York, 1997; (*f*) J. E. Anthony, *Chem. Rev.*, 2006, **106**, 5028–5048; (*g*) H. Usta, C. Risko, Z. Wang, H. Huang, M. K. Deliomeroglu, A. Zhukhovitskiy, A. Facchetti and T. J. Marks, *J. Am. Chem. Soc.*, 2009, **131**, 5586–8608; (*h*) K. Kawaguchi, K. Nakano and K. Nozaki, *J. Org. Chem.*, 2007, **72**, 5119–5128; (*i*) K.-T. Wong, T.-C. Chao, L.-C. Chi, Y.-Y. Chu, A. Balaiah, S.-F. Chiu, Y.-H. Liu and Y. Wang, *Org. Lett.*, 2006, **8**, 5033–5036; (*j*) E. Ahmed, T. Earmme, G. Q. Ren and S A. Jenekhe, *Chem. Mater.*, 2010, **22**, 5786–5796; (*k*) S. Yamaguchi, C. H. Xu and K. Tamao, *J. Am. Chem. Soc.*, 2003, **125**, 13662–13663.

2 (*a*) K. Xiao, Y. Q. Liu, T. Qi, W. Zhang, F. Wang, J. H. Gao, W. F. Qiu, Y. Q. Ma, G. L. Cui, S. Y. Chen, X. W. Zhan, G. Yu, J. G. Qin, W. P. Hu and D. B. Zhu, *J. Am. Chem. Soc.*, 2005, **127**, 13281–13286; (*b*) Q. F. Yan, Y. Zhou, B.-B. Ni, Y. G. Ma, J. Wang, J. Pei and Y. Cao, *J. Org. Chem.*, 2008, **73**, 5328–5339; (*c*) T. Izawa, E. Miyazaki and K. Takimiya, *Chem. Mater.*, 2009, **21**, 903–912; (*d*) K. Takimiya, H. Ebata, K. Sakamoto, T. Izawa, T. Otsubo and Y. Kunugi, *J. Am. Chem. Soc.*, 2006, **128**, 12604–12605; (*e*) X. Zhang, A. P. Cote and A. J. Matzger, *J. Am. Chem. Soc.*, 2005, **127**, 10502–10503; (*f*) I. Afonina, P. J. Skabara, F. Vilela, A. L. Kanibolotsky, J. C. Forgie, A. K. Bansal, G. A. Turnbull, I. D. W. Samuel, J. G. Labram, T. D. Anthopoulos, S. J. Coles and M. B. Hursthouse, *J. Mater. Chem.*, 2010, **20**, 1112–1116; (*g*) C. Hunziker, X. Zhan, P. A. Losio, H. Figi, O.-P. Kwon, S. Barlow, P. Günter and S. R. Marder, *J. Mater. Chem.*, 2007, **17**, 4972–4979.

3 (*a*) H. Usta, G. Lu, A. Facchetti and T. J. Marks, *J. Am. Chem. Soc.*, 2006, **128**, 9034–9035; (*b*) H. H. Fong, V. A. Pozdin, A. Amassian, G. G. Malliaras, D.-M. Smilgies, M. He, S. Gasper, F. Zhang and M. Sorensen, *J. Am. Chem. Soc.*, 2008, **130**, 13202–13203; (*c*) J.-Y. Wang, S. K. Hau, H.-L. Yip, J. A. Davies, K.-S. Chen, Y. Zhang, Y. Sun and A. K.-Y. Jen, *Chem. Mater.*, 2011, **23**, 765–767; (*d*) J. H. Hou, H.-Y. Chen, S. Q. Zhang, G. Li and Y. Yang, *J. Am. Chem. Soc.*, 2008, **130**, 16144–16145; (*e*) Y. Y. Liang, D. Q. Feng, Y. Wu, S.-T. Tsai, G. Li, C. Ray and L. P. Yu, *J. Am. Chem. Soc.*, 2009, **131**, 7792–7799; (*f*) S. Q. Xiao, A. C. Stuart, S. B. Liu, H. X. Zhou and W. You, *Adv. Funct. Mater.*, 2010, **20**, 635–643; (*g*) M. Q. He, J. F. Li, M. L. Sorensen, F. X.

Zhang, R. R. Hancock, H. H. Fong, V. A. Pozdin, D.-M. Smilgies and G. G. Malliaras, *J. Am. Chem. Soc.*, 2009, **131**, 11930–11938.
4 M. Q. He and F. X. Zhang, *J. Org. Chem.*, 2007, **72**, 442–451.
5 J.-H. Wan, W.-F. Fang, Z.-F. Li, X.-Q. Xiao, Z. Xu, Y. Deng, L.-H. Zhang, J.-X. Jiang, H.-Y. Qiu, L.-B. Wu and G.-Q. Lai, *Chem.–Asian J.*, 2010, **5**, 2290–2296.
6 (*a*) T. Baumgartner and R. Réau, *Chem. Rev.*, 2006, **106**, 4681–4727; (*b*) A. Saito, T. Miyajima, M. Nakashima, T. Fukushima, H. Kaji, Y. Matano and H. Imahori, *Chem.–Eur. J.*, 2009, **15**, 10000–10004; (*c*) Y. Dienes, M. Eggenstein, T. Kárpáti, T. Sutherland, L. Nyulászi and T. Baumgartner, *Chem.–Eur. J.*, 2008, **14**, 9878–9889; (*d*) Y. Dienes, S. Durben, T. K-rp-ti, T. Neumann, U. Englert, L. Nyul-szi and T. Baumgartner, *Chem.–Eur. J.*, 2007, **13**, 7487–7500; (*e*) A. Fukazawa, Y. Ichihashi, Y. Kosaka and S. Yamaguchi, *Chem.–Asian J.*, 2009, **4**, 1729–1740; (*f*) C. Fave, T. Y. Cho, M. Hissler, C. W. Chen, T. Y. Luh, C. C. Wu and R. Réau, *J. Am. Chem. Soc.*, 2003, **125**, 9254–9255; (*g*) T. Baumgartner, W. Bergmans, T. Kárpáti, T. Neumann, M. Nieger and L. Nyulászi, *Chem.–Eur. J.*, 2005, **11**, 4687–4699; (*h*) J. Crassous and R. Réau, *Dalton Trans.*, 2008, 6865–6876; (*i*) O. Fadhel, Z. Benkö, M. Gras, V. Deborde, D. Joly, C. Lescop, L. Nyulászi, M. Hissler and R. Réau, *Chem.–Eur. J.*, 2010, **16**, 11340–11356; (*j*) T. Miyajima, Y. Matano and H. Imahori, *Eur. J. Org. Chem.*, 2008, **2**, 255–259.
7 (*a*) E. W. Meijer and A. P. H. J. Schenning, *Nature*, 2002, **419**, 353–354; (*b*) F. Würthner, *S. D. Supramolecular Dye Chemistry*, Springer-Verlag, Heidelberg, 2005; (*c*) J. Elemans, A. E. Rowan and R. J. M. Nolte, *J. Mater. Chem.*, 2003, **13**, 2661–2670; (*d*) L. A. Estroff and A. D. Hamilton, *Chem. Rev.*, 2004, **104**, 1201–1218; (*e*) S. I. Stupp, V. Le Bonheur, K. Walker, L. S. Li, K. Huggins, M. Keser and A. Amstutz, *Science*, 1997, **276**, 384–389; (*f*) K. Ariga, T. Nakanishi and J. P. Hill, *Curr. Opin. Colloid Interface Sci.*, 2007, **12**, 106–120; (*g*) L. Zang, Y. Che and J. S. Moore, *Acc. Chem. Res.*, 2008, **41**, 1596; (*h*) J. P. Hill, W. Jin, A. Kosaka, T. Fukushima, H. Ichihara, T. Shimomura, K. Ito, T. Hashizume, N. Ishii and T. Aida, *Science*, 2004, **304**, 1481.
8 (*a*) K. Müllen, G. Wegner, *Electronic Materials: The Oligomer Approach*, Wiley-VCH, Weinheim, 1998; (*b*) V. Percec, M. Glodde, T. K. Bera, Y. Miura, I. Shiyanovskaya, K. D. Singer, V. S. K. Balagurusamy, P. A. Heiney, I. A. Schnell, H.-W. Spiess, S. D. Hudsonk and H. Duank, *Nature*, 2002, **417**, 384–387; (*c*) F. J. M. Hoeben, P. Jonkheijm, E. W. Meijer and A. P. H. Schenning, *Chem. Rev.*, 2005, **105**, 1491–1546; (*d*) S. Banerjee, R. K. Das and U. Maitra, *J. Mater. Chem.*, 2009, **19**, 6649–6687; (*e*) J.-M. Lehn, J. L. Atwood, J. E. D. Davies, D. D. MacNicol, F. Vogtle, *Comprehensive Supramolecular Chemistry*, Pergamon, New York, 1996; (*f*) G.-R. David and P. H. J. Albertus, *Chem. Mater.*, 2011, **23**, 310–325.
9 (*a*) M. George and R. G. Weiss, *Acc. Chem. Res.*, 2006, **39**, 489; (*b*) A. Ajayaghosh and V. K. Praveen, *Acc. Chem. Res.*, 2007, **40**, 644–656; (*c*) T. Kato, Y. Hirai, S. Nakaso and M. Moriyama, *Chem. Soc. Rev.*, 2007, **36**, 1857–1867; (*d*) H. Maeda, *Chem.–Eur. J.*, 2008, **14**, 11274–11282; (*e*) S. Diring, F. Camerel, B. Donnio, T. Dintzer, S. Toffanin, R. Capelli, M. Muccini and R. Ziessel, *J. Am. Chem. Soc.*, 2009, **131**, 18177–18185; (*f*) J. Wu, T. Yi, T. Shu, M. X. Yu, Z. G. Zhou, M. Xu, Y. F. Zhou, H. J. Zhang, J. T. Han, F. Y. Li and C. H. Huang, *Angew. Chem., Int. Ed.*, 2008, **47**, 1063–1067; (*g*) Y. Li, K. Liu, J. Liu, J. Peng, X. Feng and Y. Fang, *Langmuir*, 2006, **22**, 7016–7020; (*h*) T. Y. Wang, Y. G Li and M. H. Liu, *Soft Matter*, 2009, **5**, 1066–1073; (*i*) P. C. Xue, R. Lu, G. J. Chen, Y. Zhang, H. Nomoto, M. Takafuji and H. Ihara, *Chem.–Eur. J.*, 2007, **13**, 8231–8239; (*j*) D. F. Xu, X. L. Liu, R. Lu, P. C. Xue, X. F. Zhang, H. P. Zhou and J. H. Jia, *Org. Biomol. Chem.*, 2011, **9**, 1523–1528; (*k*) *Gels and Fibrillar Networks Preface,Langmuir*, 2009, **25**, 8369–8840.
10 (*a*) M. Shirakawa, N. Fujita and S. Shinkai, *J. Am. Chem. Soc.*, 2005, **127**, 4614–4615; (*b*) C. Wang, Q. Chen, F. Sun, D. Q. Zhang, G. X. Zhang, Y. Y. Huang, R. Zhao and D. B. Zhu, *J. Am. Chem. Soc.*, 2010, **132**, 3092–3096; (*c*) W. J. Kim, B. M. Jung, S. H. Kang and J. Y. Chang, *Soft Matter*, 2011, **7**, 4160–4162; (*d*) G. AndreDel, G. L. Alexandre, Olive, J. Reichwagen, H. Hopf and J.-P. Desvergne, *J. Am. Chem. Soc.*, 2005, **127**, 17984–17985; (*e*) S. Wang, W. Shen, Y. L. Feng and H. Tian, *Chem. Commun.*, 2006, 1497–1499; (*f*) J. W. Chung, B. K. An and S. Y. Park, *Chem. Mater.*, 2008, **20**, 6750–6755; (*g*) A. Dawn, N. Fujita, S. Haraguchi, K. Sada, S.-i. Tamaru and S. Shinkai, *Org. Biomol. Chem.*, 2009, **7**, 4378–4385; (*h*) J.-H. Wan, L.-Y. Mao, Y.-B. Li, Z.-F. Li, H.-Y. Qiu, C. Wang and G.-Q. Lai, *Soft Matter*, 2010, **6**, 3195–3201.
11 (*a*) S. Xiao, J. Tang, T. Beetz, X. Guo, N. Tremblay, T. Siegrist, Y. Zhu, M. Steigerwald and C. Nuckolls, *J. Am. Chem. Soc.*, 2006, **128**, 10700–10701; (*b*) A. L. Briseno, M. Roberts, M.-M. Ling, H. Moon, E. J. Nemanick and Z. Bao, *J. Am. Chem. Soc.*, 2006, **128**, 3880–3881; (*c*) A. L. Briseno, S. C. B. Mannsfeld, X. Lu, Y. Xiong, S. A. Jenekhe, Z. Bao and Y. Xia, *Nano Lett.*, 2007, **7**, 668–675; (*d*) J.-P. Hong, M.-C. Um, S.-R. Nam, J.-I. Hong and S. Lee, *Chem. Commun.*, 2009, 310–312; (*e*) Y. Zhou, W.-J. Liu, Y. Ma, H. Wang, L. Qi, Y. Cao, J. Wang and J. Pei, *J. Am. Chem. Soc.*, 2007, **129**, 12386.
12 (*a*) L. Schmidt-Mende, A. Fechtenkötter, K. Müllen, E. Moons, R. H. Friend and J. D. MacKenzie, *Science*, 2001, **293**, 1119–1122; (*b*) X. Yang, J. Loos, S. C. Veenstra, W. J. H. Verhees, M. M. Wienk, J. M. Kroon, M. A. J. Michels and R. A. J. Janssen, *Nano Lett.*, 2005, **5**, 579–583; (*c*) S. Berson, R. De Bettignies, S. Bailly and S. Guillerez, *Adv. Funct. Mater.*, 2007, **17**, 1377–1384.
13 B. Zhao, B. Liu, R. Q. Png, K. Zhang, K. A. Lim, J. Luo, J. J. Shao, K. H. H. Peter, C. Y. Chi and J. H. Wu, *Chem. Mater.*, 2010, **22**, 435–449.
14 (*a*) S. H. Yan, S. J. Lee, S. W. Kang, K. H. Choi, S. K. Rhee and J. Y. Lee, *Bull. Korean Chem. Soc.*, 2007, **28**, 959–964; (*b*) C.-Q. Wan, J. Han and C. W. Thomas, *New J. Chem.*, 2009, **33**, 707–712.
15 (*a*) S.-T. Lam, G. X. Wang and V. W.-W. Yam, *Organometallics*, 2008, **27**, 4545–4548; (*b*) D. D. Diaz, T. Torres, R. Zentel, R. Davis and M. Brehmer, *Chem. Commun.*, 2007, 2369–2371.
16 (*a*) X. Huang, S. R. Raghavan, P. Terech and R. G. Weiss, *J. Am. Chem. Soc.*, 2006, **128**, 15341–15352; (*b*) X. Huang, P. Terech, S. R. Raghavan and R. G. Weiss, *J. Am. Chem. Soc.*, 2005, **127**, 4336–4344; (*c*) G. Tan, V. T. John and G. L. McPherson, *Langmuir*, 2006, **22**, 7416–7420; (*d*) J. L. Li, B. Yuan, X. Y. Liu and H. Y. Xu, *Cryst. Growth. Des*, 2010, **10**, 2069–2706.
17 M. Lescanne, A. Colin, O. Mondain-Monval, F. Fages and J. L. Pozzo, *Langmuir*, 2003, **19**, 2013–2020.
18 (*a*) A. S. Davydov, *Theory of Molecular Excitons*, Plenum Press, New York, 1971; (*b*) E. H. A. Beckers, S. C. J. Meskers, A. P. H. J. Schenning, Z. J. Chen, F. Würthner, P. Marsal, D. Beljonne, J. Cornil and R. A. J. Janssen, *J. Am. Chem. Soc.*, 2006, **128**, 649; (*c*) F. Würthner, C. Bauer, V. Stepanenko and S. Yagai, *Adv. Mater.*, 2008, **20**, 1695–1698; (*d*) S. Abraham, K. Ratheesh, R. K. Vijayaraghavan and S. Das, *Langmuir*, 2009, **25**, 8507–8513; (*e*) T. E. Kaiser, V. Stepanenko and F. Würthner, *J. Am. Chem. Soc.*, 2009, **131**, 6719–6732.
19 *Gaussian 03, Revision B.04*, M. J. Frisch, G. W. Trucks, H. B. Schlegel, G. E. Scuseria, M. A. Robb, J. R. Cheeseman, J. A. Montgomery, Jr., T. Vreven, K. N. Kudin, J. C. Burant, J. M. Millam, S. S. Iyengar, J. Tomasi, V. Barone, B. Mennucci, M. Cossi, G. Scalmani, N. Rega, G. A. Petersson, H. Nakatsuji, M. Hada, M. Ehara, K. Toyota, R. Fukuda, J. Hasegawa, M. Ishida, T. Nakajima, Y. Honda, O. Kitao, H. Nakai, M. Klene, X. Li, J. E. Knox, H. P. Hratchian, J. B. Cross, V. Bakken, C. Adamo, J. Jaramillo, R. Gomperts, R. E. Stratmann, O. Yazyev, A. J. Austin, R. Cammi, C. Pomelli, J. W. Ochterski, P. Y. Ayala, K. Morokuma, G. A. Voth, P. Salvador, J. J. Dannenberg, V. G. Zakrzewski, S. Dapprich, A. D. Daniels, M. C. Strain, O. Farkas, D. K. Malick, A. D. Rabuck, K. Raghavachari, J. B. Foresman, J. V. Ortiz, Q. Cui, A. G. Baboul, S. Clifford, J. Cioslowski, B. B. Stefanov, G. Liu, A. Liashenko, P. Piskorz, I. Komaromi, R. L. Martin, D. J. Fox, T. Keith, M. A. Al-Laham, C. Y. Peng, A. Nanayakkara, M. Challacombe, P. M. W. Gill, B. Johnson, W. Chen, M. W. Wong, C. Gonzalez and J. A. Pople, Gaussian, Inc., Wallingford, CT, 2004.
20 (*a*) F. Wüthner, S. Yao and U. Beginn, *Angew. Chem., Int. Ed.*, 2003, **42**, 3247–3250; (*b*) J. Mamiya, K. Kanie, T. Hiyama, T. Ikeda and T. Kato, *Chem. Commun.*, 2002, 1870–1871; (*c*) B. K. An, D. S. Lee, J. S. Lee, Y. S. Park, H. S. Song and S. Y. Park, *J. Am. Chem. Soc.*, 2004, **126**, 10232–10233; (*d*) L. J. Zhi, J. S. Wu and K. Müllen, *Org. Lett.*, 2005, **7**, 5761–5764; (*e*) D. C. Lee, K. K. McGrath and K. Jang, *Chem. Commun.*, 2008, 3636–3638; (*f*) T. Haino, M. Tanaka and Y. Fukazawa, *Chem. Commun.*, 2008, 468–470; (*g*) S. Varghese, S. Nambalan, S. Kumar, A. Krishna, S. Doddamane, S. Rao, S. K. Prasad and S. Das, *Adv. Funct. Mater.*, 2009, **19**, 2064.
21 (*a*) S. De Feyter, A. Gesquière, M. M. Abdel-Mottaleb, C. M. Grim, C. De Schryver, C. Meiners, M. Sieffert, S. Valiyaveettil and K. Müllen, *Acc. Chem. Res.*, 2000, **33**, 520–531; (*b*) S. De Feyter and F. C. De Schryver, *Chem. Soc. Rev.*, 2003, **32**, 139–150; (*c*) L. Wan, *Acc. Chem. Res.*, 2006, **39**, 334–342.
22 (*a*) J. P. Rabe and S. Buchholz, *Science*, 1991, **253**, 424; (*b*) S. L. Xu, Q. D. Zeng, P. Wu, Y. H. Qiao, C. Wang and C. L. Bai, *Appl. Phys. A: Mater. Sci. Process.*, 2003, **76**, 209; (*c*) T. Nakanishi, N. Miyashita, T. Michinobu, Y. Wakayama, T. Tsuruoka, K. Ariga and D. G. Kurth, *J. Am. Chem. Soc.*, 2006, **128**, 6328–6329.

